Figure S1

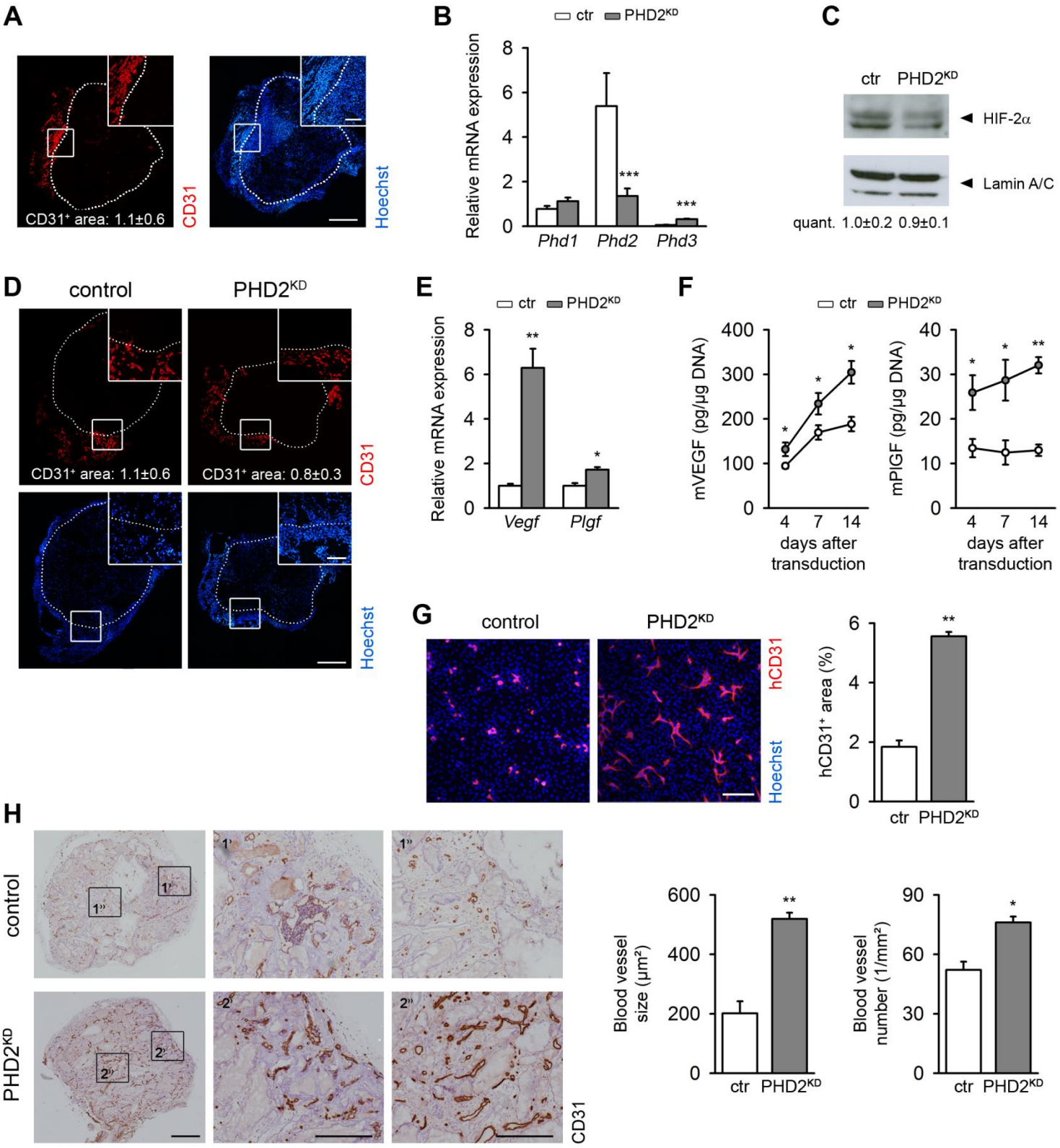
A
CD31⁺ area: 1.1±0.6
CD31
Hoechst
B
ctr
PHD2KD
Relative mRNA expression
Phd1
Phd2
Phd3
***
***
C
ctr
PHD2KD
HIF-2α
Lamin A/C
quant. 1.0±0.2 0.9±0.1
D
control
PHD2KD
CD31⁺ area: 1.1±0.6
CD31⁺ area: 0.8±0.3
CD31
Hoechst
E
ctr
PHD2KD
Relative mRNA expression
Vegf
Plgf
F
ctr
PHD2KD
mVEGF (pg/µg DNA)
mPlGF (pg/µg DNA)
days after transduction
days after transduction
G
control
PHD2KD
hCD31
Hoechst
hCD31⁺ area (%)
H
control
PHD2KD
CD31
Blood vessel size (µm²)
Blood vessel number (1/mm²)

Figure S1, Related to Figure 1. PHD2 Silencing Increases Angiogenesis at Late, But Not at Early Time Points

(A) CD31 immunostaining of mouse periosteal cell-seeded scaffolds, with quantification of the $CD31^+$ area inside the scaffold (n=4). Boxed areas are subsequently magnified.

(B) *Phd1*, *Phd2* and *Phd3* mRNA levels in cultured control (ctr) and $PHD2^{KD}$ periosteal cells three days after transduction, analyzed by qRT-PCR (n=6).

(C) Western blot analysis of HIF-2α and Lamin A/C on nuclear fractions. The ratio of HIF-2α to Lamin A/C is quantified (quant.; n=3) and representative blots are shown.

(D) CD31 immunostaining with a higher magnification of the boxed area. $CD31^+$ area inside the scaffold was quantified (n=4).

(E) Relative *Vegf* and *Plgf* mRNA levels, analyzed by qRT-PCR (n=6).

(F) VEGF (left graph) and PlGF (right graph) protein levels in conditioned medium, analyzed at indicated time points by ELISA (n=3).

(G) Immunostaining images and quantification of human CD31 (hCD31)-positive surface of periosteal cells cocultured with human umbilical vein endothelial cells (scale bar, 500 µm; n=6).

(H) CD31 immunostaining on ectopically implanted scaffolds eight weeks after implantation, with quantification of blood vessel size and number, analyzed in the entire scaffold (n=6). Boxed areas are subsequently magnified.

Data are means ± SEM. *p<0.05 vs. ctr, **p<0.01 vs. ctr, ***p<0.001 vs. ctr (Student's *t*-test).

Figure S2

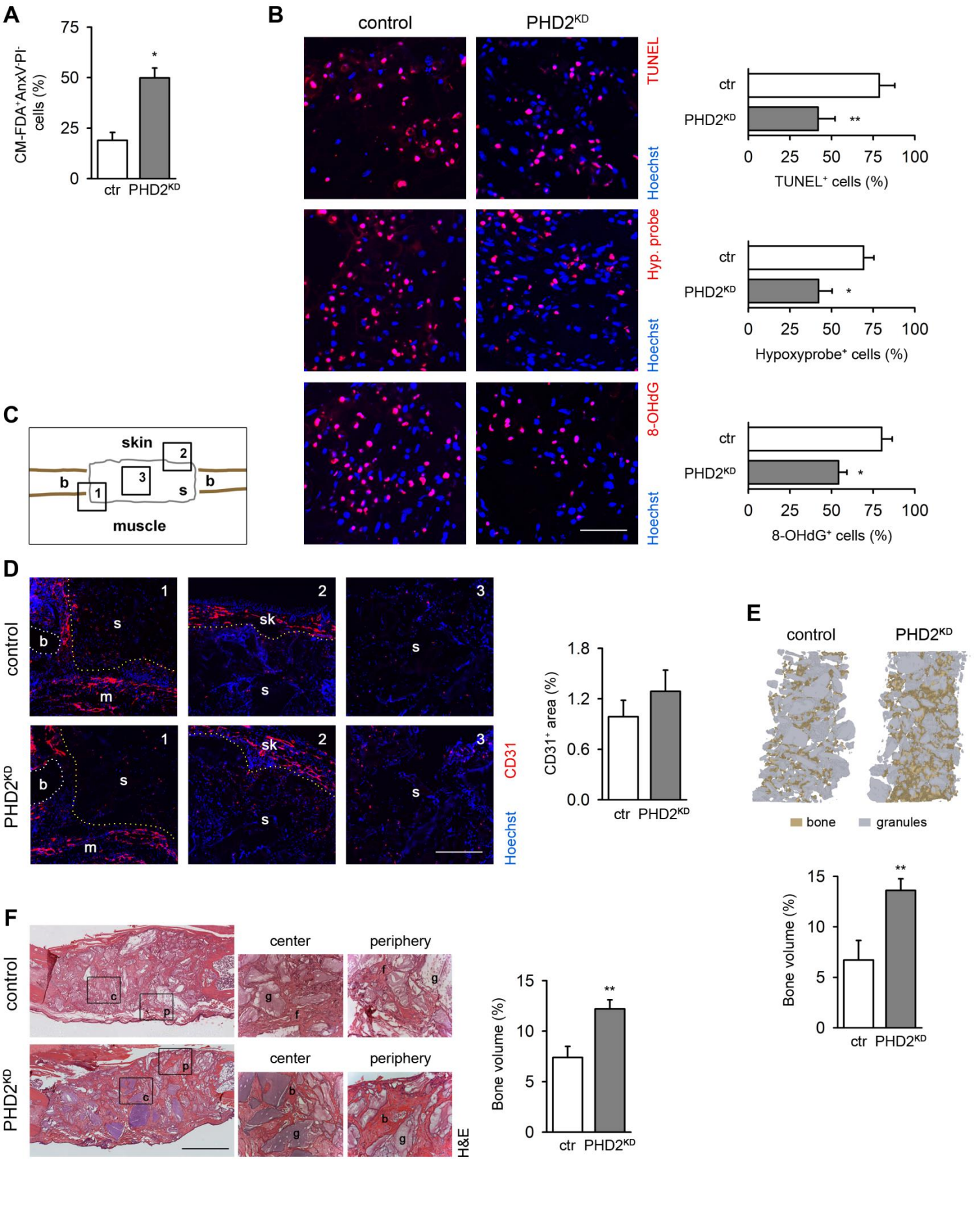
A
CM-FDA+AnxV-PI- cells (%)
ctr
PHD2KD
B
control
PHD2KD
TUNEL
Hoechst
Hyp. probe
8-OHdG
TUNEL+ cells (%)
Hypoxyprobe+ cells (%)
8-OHdG+ cells (%)
C
skin
muscle
b
s
D
control
PHD2KD
CD31
CD31+ area (%)
E
bone
granules
Bone volume (%)
F
center
periphery
H&E

Figure S2, Related to Figure 1. Silencing PHD2 Improves Cell Survival and Bone Regeneration in a Large Bone Defect Model

(A) *Ex vivo* AnxV-PI flow cytometry analysis, with quantification of the viable implanted CM-FDA^{+}AnxV^{-}PI^{-} cells (n=3).

(B) TUNEL, hypoxyprobe (Hyp. probe) and 8-OHdG immunostaining with quantification of TUNEL^{+}, hypoxyprobe^{+} and 8-OHdG^{+} cells in the scaffold center (n=3).

(C) Schematic representation of large bone defect (b, bone; s, scaffold).

(D) CD31 immunostaining with quantification of CD31^{+} area inside the scaffold. Numbering of pictures in panel E corresponds to schematic representation (C). Yellow dotted lines indicate scaffold boundaries (b, bone; sk, skin; s, scaffold).

(E-F) Quantification of newly formed bone by micro-computed tomography-based 3D visualization (E) and H&E staining (F), analyzed on the entire scaffold (n=4). Boxed areas are subsequently magnified (c, central region; p, periphery; b, bone; f, fibrous tissue; g, scaffold granule).

For A,B and D, analysis was performed at day three after implantation; for E and F, analysis was performed eight weeks after implantation. Scale bars are 100 µm in B; 250 µm in D; and 1 mm in F. Data are means ± SEM. *p<0.05 vs. ctr, **p<0.01 vs. ctr (Student's *t*-test).

Figure S3

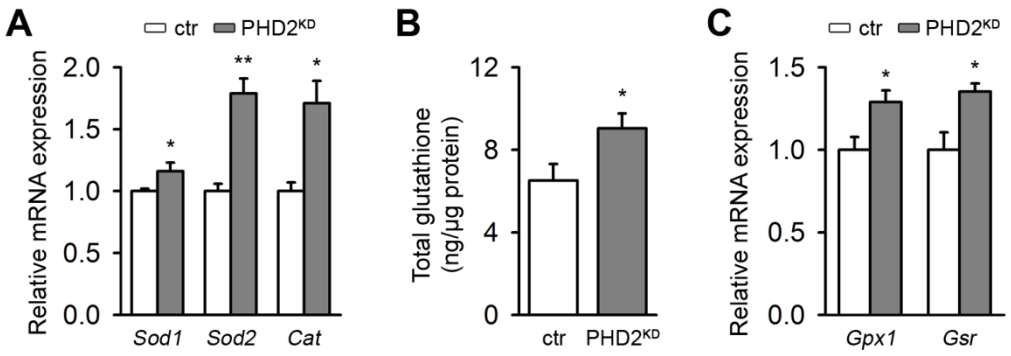

Figure S3, Related to Figure 2. Silencing of PHD2 Increases Antioxidant Levels

(A) Relative *Sod1*, *Sod2* and *Cat* mRNA levels of cultured control (ctr) and PHD2^{KD} periosteal cells, analyzed by qRT-PCR (n=6).

(B) Total glutathione levels in cultured periosteal cells (n=6).

(C) Relative *Gpx1* and *Gsr* mRNA levels, analyzed by qRT-PCR (n=6).

Data are means ± SEM. *p<0.05 vs. ctr, **p<0.01 vs. ctr (Student's *t*-test).

Figure S4

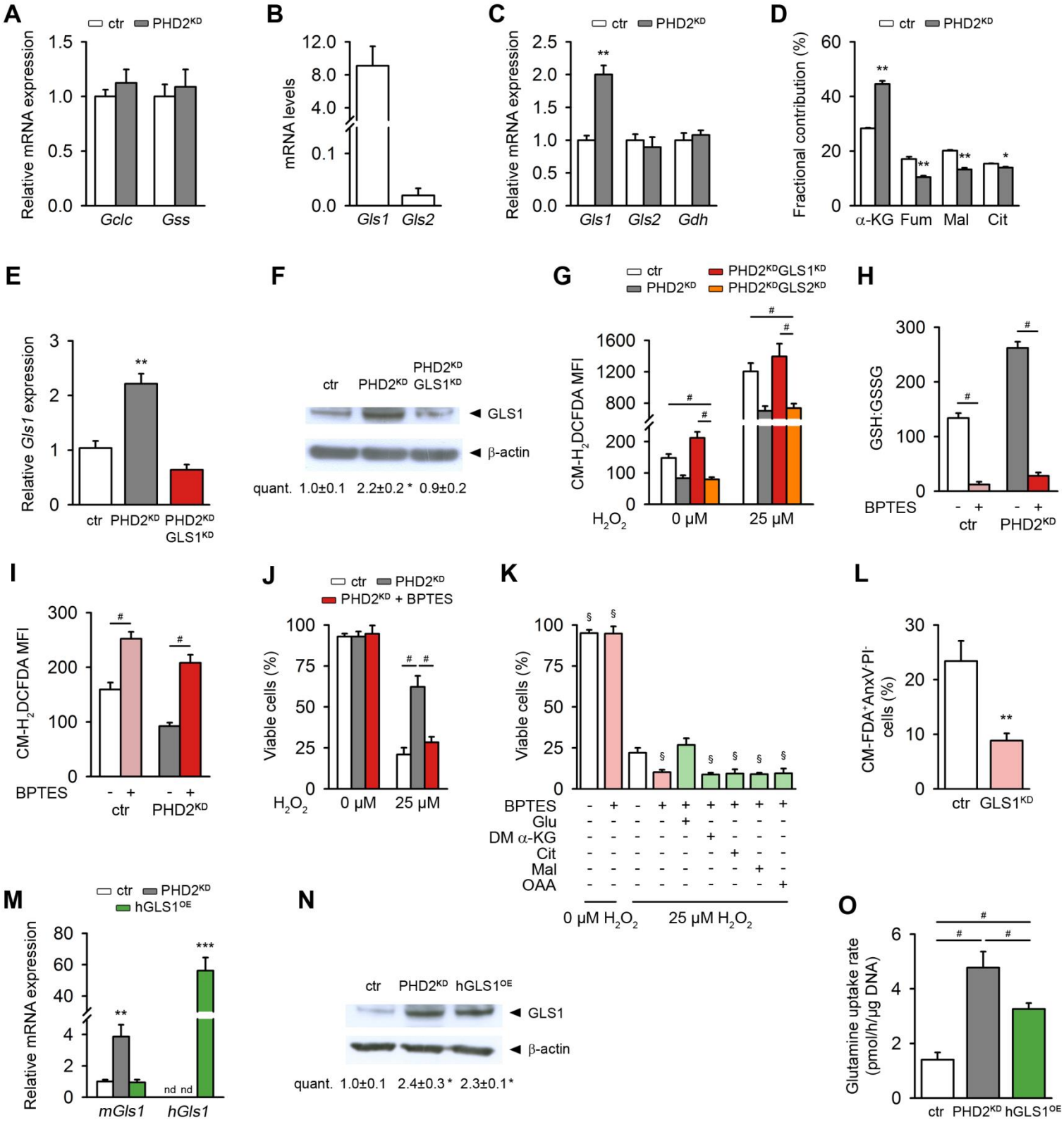
A
ctr
PHD2KD
Relative mRNA expression
Gclc
Gss
B
mRNA levels
Gls1
Gls2
C
Relative mRNA expression
Gls1
Gls2
Gdh
D
Fractional contribution (%)
α-KG
Fum
Mal
Cit
E
Relative Gls1 expression
ctr
PHD2KD
PHD2KD GLS1KD
F
PHD2KD GLS1KD
GLS1
β-actin
quant. 1.0±0.1 2.2±0.2 * 0.9±0.2
G
PHD2KDGLS1KD
PHD2KDGLS2KD
CM-H2DCFDA MFI
H2O2
0 μM
25 μM
H
GSH:GSSG
BPTES
I
CM-H2DCFDA MFI
J
PHD2KD + BPTES
Viable cells (%)
K
L
CM-FDA+AnxV-PI- cells (%)
GLS1KD
M
hGLS1OE
Relative mRNA expression
mGls1
hGls1
nd nd
N
hGLS1OE
quant. 1.0±0.1 2.4±0.3 * 2.3±0.1 *
O
Glutamine uptake rate (pmol/h/μg DNA)

Figure S4, Related to Figure 3. GLS1 is Necessary for Glutathione-Mediated ROS Scavenging in PHD2^{KD} Cells

(A) Relative *Gclc* and *Gss* mRNA levels of cultured control (ctr) and PHD2^{KD} periosteal cells, analyzed by qRT-PCR (n=6).

(B) *Gls1* and *Gls2* mRNA levels in cultured wild-type periosteal cells, analyzed by qRT-PCR (n=6).

(C) Relative *Gls1*, *Gls2* and *Gdh* mRNA levels, analyzed by qRT-PCR (n=6).

(D) Fractional contribution of [U-^{13}C]-glutamine to α-ketoglutarate (α-KG), fumarate (Fum), malate (Mal) and citrate (Cit).

(E) Relative *Gls1* mRNA levels analyzed by qRT-PCR after transduction with scrambled (ctr, PHD2^{KD}) or GLS1 shRNA (PHD2^{KD}GLS1^{KD}) (n=6).

(F) Western blot analysis of GLS1 and β-actin after shRNA-mediated silencing of GLS1. Ctr and PHD2^{KD} cells are transduced with scrambled shRNA. The ratio of GLS1 to β-actin is quantified (quant.; n=3) and representative blots are shown.

(G) Total intracellular ROS levels via CM-H_2DCFDA flow cytometry in control and PHD2^{KD} cells after silencing of GLS1 or GLS2 with or without treatment with 25 µM H_2O_2 (n=6). PHD2^{KD}GLS1^{KD} and PHD2^{KD}GLS2^{KD} cells are PHD2^{KD} cells transduced with shGLS1 or shGLS2, respectively; ctr and PHD2^{KD} cells are transduced with shScr.

(H-I) Ratio of reduced glutathione (GSH) to oxidized glutathione (GSSG) levels (H) and total intracellular ROS levels analyzed by CM-H_2DCFDA flow cytometry (I) in control and PHD2^{KD} cells after pharmacological inhibition of GLS1 with BPTES (n=6).

(J) Analysis of cell viability of control, PHD2^{KD} and BPTES-treated PHD2^{KD} cells after treatment with 25 µM H_2O_2, using AnxV-PI flow cytometry (n=6).

(K) Rescue of viability of BPTES-treated control cells during oxidative stress (25 µM H_2O_2) with glutamate (Glu), but not with dimethyl α-ketoglutarate (DM α-KG), citrate (Cit), malate (Mal) or oxaloacetate (OAA), evidenced by AnxV-PI flow cytometry (n=3).

(L) *Ex vivo* AnxV-PI flow cytometry analysis of viable CM-FDA^{+}AnxV^{-}PI^{-} control and GLS1-silenced cells (GLS1^{KD}), three days after *in vivo* implantation (n=3-4).

(M) Relative mouse (*m*)*Gls1* and human (*h*)*Gls1* mRNA levels in control, PHD2^{KD} and hGLS1 overexpressing (hGLS1^{OE}) cells, analyzed by qRT-PCR (nd is not determined; n=6).

(N) Western blot analysis of GLS1 and β-actin in control, PHD2^{KD} and hGLS1^{OE} cells. The ratio of GLS1 to β-actin is quantified (quant.; n=3) and representative blots are shown.

(O) Glutamine uptake rate in control, PHD2^{KD} and hGLS1^{OE} cells (n=6).

Data are means ± SEM. *p<0.05 vs. ctr, **p<0.01 vs. ctr, ***p<0.001 vs. ctr, §p<0.05 vs. H_2O_2-treated ctr cells (Student's *t*-test), $^{\#}$p<0.05 (ANOVA).

Figure S5

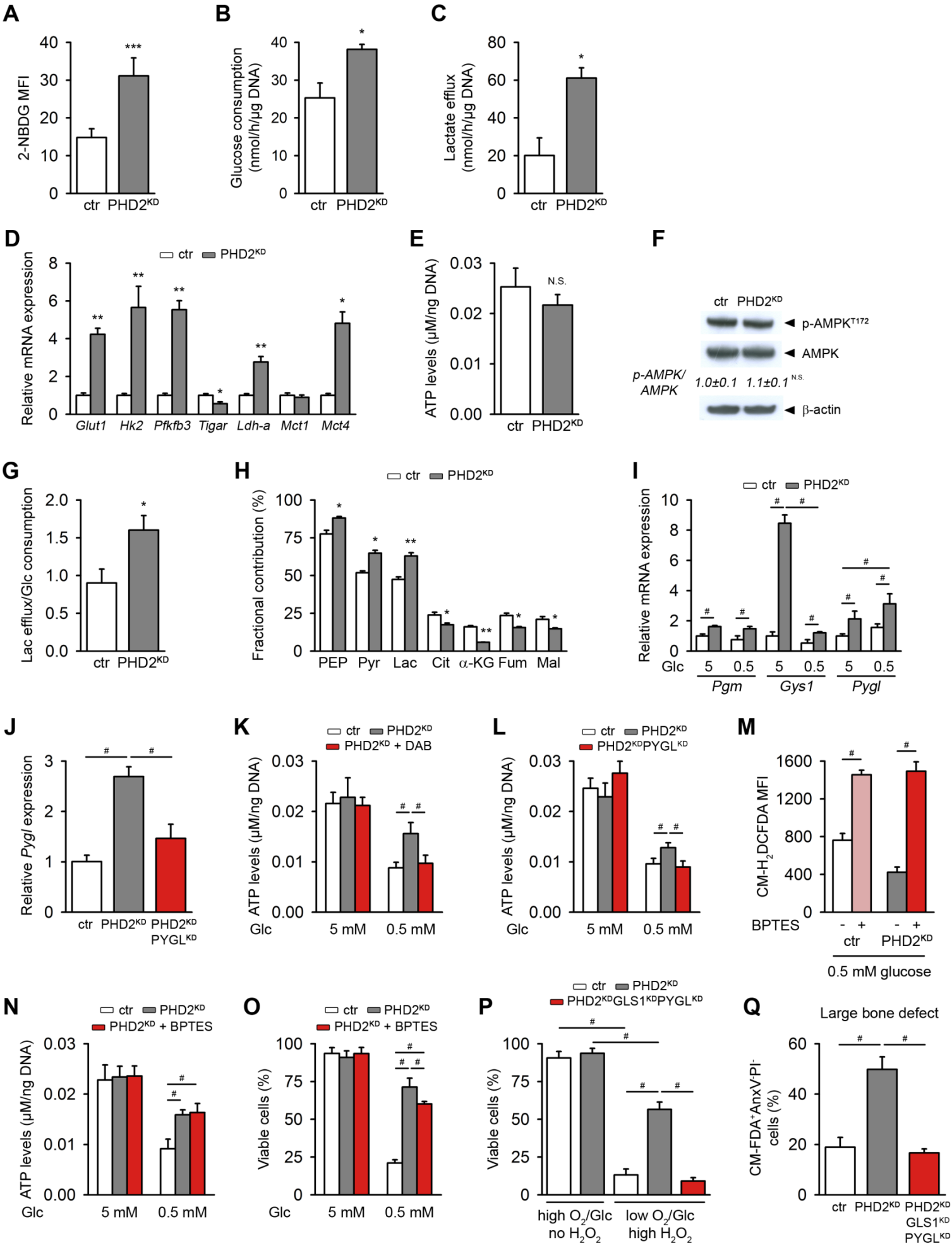
A
2-NBDG MFI
ctr
PHD2KD
B
Glucose consumption (nmol/h/µg DNA)
C
Lactate efflux (nmol/h/µg DNA)
D
Relative mRNA expression
Glut1
Hk2
Pfkfb3
Tigar
Ldh-a
Mct1
Mct4
E
ATP levels (µM/ng DNA)
N.S.
F
p-AMPKT172
AMPK
p-AMPK/ AMPK
1.0±0.1
1.1±0.1
β-actin
G
Lac efflux/Glc consumption
H
Fractional contribution (%)
PEP
Pyr
Lac
Cit
α-KG
Fum
Mal
I
Relative mRNA expression
Glc
Pgm
Gys1
Pygl
J
Relative Pygl expression
PHD2KD PYGLKD
K
PHD2KD + DAB
ATP levels (µM/ng DNA)
5 mM
0.5 mM
L
PHD2KDPYGLKD
M
CM-H2DCFDA MFI
BPTES
0.5 mM glucose
N
PHD2KD + BPTES
O
Viable cells (%)
P
PHD2KDGLS1KDPYGLKD
high O2/Glc no H2O2
low O2/Glc high H2O2
Q
Large bone defect
CM-FDA+AnxV-PI- cells (%)
PHD2KD GLS1KD PYGLKD

Figure S5, Related to Figure 4 and Figure 5. PHD2 Silencing Alters Glucose Metabolism

(A) 2-NBDG mean fluorescent intensity (MFI) as a measure of glucose uptake, analyzed by flow cytometry in cultured control (ctr) and $PHD2^{KD}$ cells (n=6).

(B-C) Glucose consumption rate (B) and lactate efflux rate (C), measured in conditioned medium (n=9).

(D) Relative *Glut1*, *Hk2*, *Pfkfb3*, *Tigar*, *Ldh-a*, *Mct1* and *Mct4* mRNA levels, analyzed by qRT-PCR (n=6).

(E) Intracellular ATP levels (N.S. is not significant, n=6).

(F) $P\text{-}AMPK^{T172}$ (phosphorylated at $Threonin^{172}$), AMPK and β-actin immunoblot, with quantification of the relative ratio of $p\text{-}AMPK^{T172}$ to total AMPK. Results are representative of three experiments (N.S. is not significant).

(G) Ratio of lactate (Lac) efflux to glucose (Glc) consumption, indicative of fermentative metabolism (n=9).

(H) Fractional contribution of [U-^{13}C]-glucose to phosphoenolpyruvate (PEP), pyruvate (Pyr), lactate (Lac), citrate (Cit), fumarate (Fum) and malate (Mal) (n=6).

(I) Relative *Pgm*, *Gys1* and *Pygl* mRNA levels during normal culture conditions (5 mM glucose) or glucose deprivation (0.5 mM glucose), analyzed by qRT-PCR (n=6).

(J) Relative *Pygl* mRNA levels analyzed by qRT-PCR after transduction with scrambled (ctr, $PHD2^{KD}$) or PYGL shRNA ($PHD2^{KD}PYGL^{KD}$) (n=6).

(K-L) Intracellular ATP levels of cells cultured during normal culture conditions or glucose deprivation (0.5 mM glucose) with or without pharmacological inhibition (with DAB; K) or genetic silencing (with shRNA; L) of PYGL in $PHD2^{KD}$ cells (n=6).

(M-O) Total intracellular ROS levels via CM-H_2DCFDA flow cytometry (M), intracellular ATP levels (N) and cell viability via Annexin V-PI flow cytometry (O) of control and $PHD2^{KD}$ cells after pharmacological inhibition of GLS1 with BPTES during glucose deprivation (0.5 mM glucose) (n=6).

(P) AnxV-PI cell viability analysis of cultured ctr cells, $PHD2^{KD}$ cells and $PHD2^{KD}$ cells with genetic inhibition of GLS1 and PYGL ($PHD2^{KD}GLS1^{KD}PYGL^{KD}$) during normal or combined stress conditions (1% oxygen (O_2), 1 mM glucose (Glc) and 12 µM H_2O_2 (high H_2O_2); n=4).

(Q) *Ex vivo* AnxV-PI flow cytometry analysis, with quantification of the viable $CM\text{-}FDA^{+}AnxV^{-}PI^{-}$ cells, after implantation for three days in a large bone defect (n=3).

Data are means ± SEM. *p<0.05 vs. ctr, **p<0.01 vs. ctr, ***p<0.001 vs. ctr (Student's *t*-test), $^{\#}$p<0.05 (ANOVA).

Figure S6

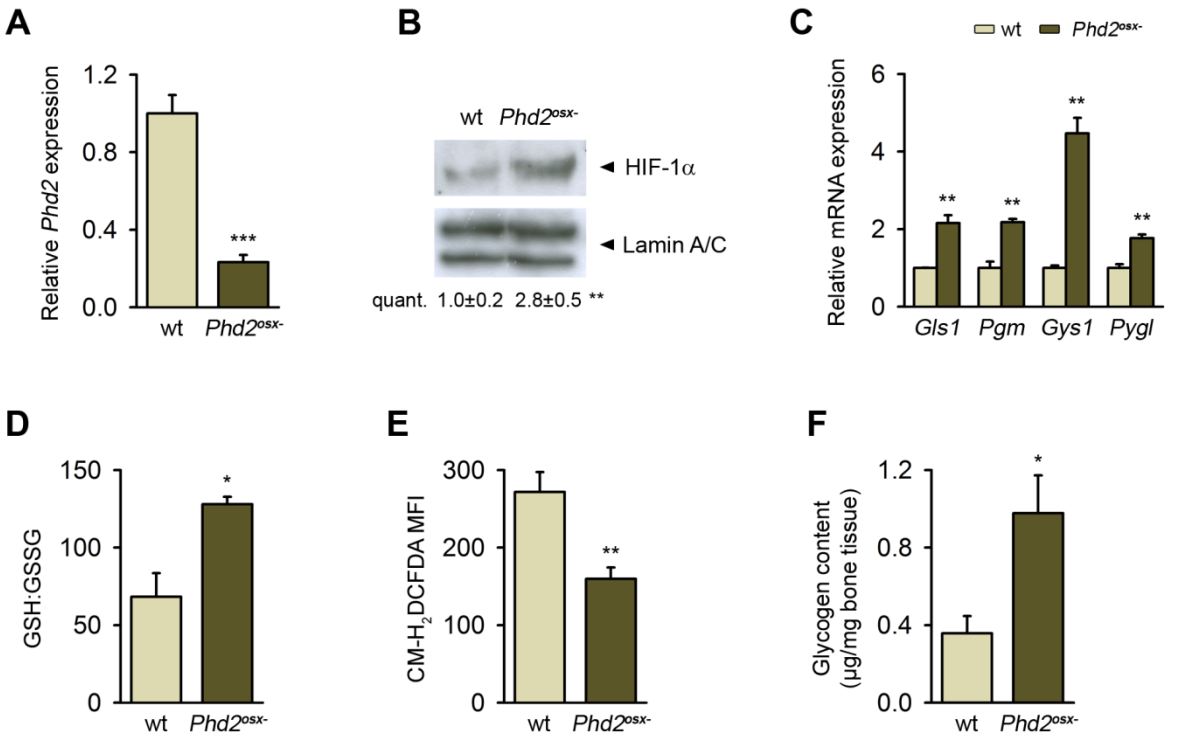

Figure S6, Related to Figure 3, Figure 4 and Figure 5. Deletion of PHD2 in Osteoprogenitors alters Glutamine and Glycogen Metabolism.

(A) *Phd2* mRNA levels in the osteogenic fraction of long bones of wild-type (wt) and Osterix-Cre mediated PHD2 knockout (*Phd2*$^{osx-}$) mice, analyzed by qRT-PCR (n=3).

(B) Western blot analysis of HIF-1α and Lamin A/C on nuclear protein fractions from osteogenic cells of long bones. The ratio of HIF-1α to Lamin A/C is quantified (quant.; n=2) and representative blots are shown.

(C) *Gls1*, *Pgm*, *Gys1* and *Pygl* mRNA levels in the osteogenic fraction of long bones, analyzed by qRT-PCR (n=3).

(D) Ratio of GSH to GSSG levels in the osteogenic fraction of long bones (n=4-5).

(E) Flow cytometry analysis of intracellular ROS levels in osteogenic cells isolated from long bones, quantified by CM-H_2DCFDA MFI (n=4-5).

(F) Intracellular glycogen levels, determined after extraction from osteogenic cells isolated from long bones (n=4-5).

Data are means ± SEM. *p<0.05 vs. ctr, **p<0.01 vs. ctr, ***p<0.001 vs. ctr (Student's *t*-test).

Figure S7

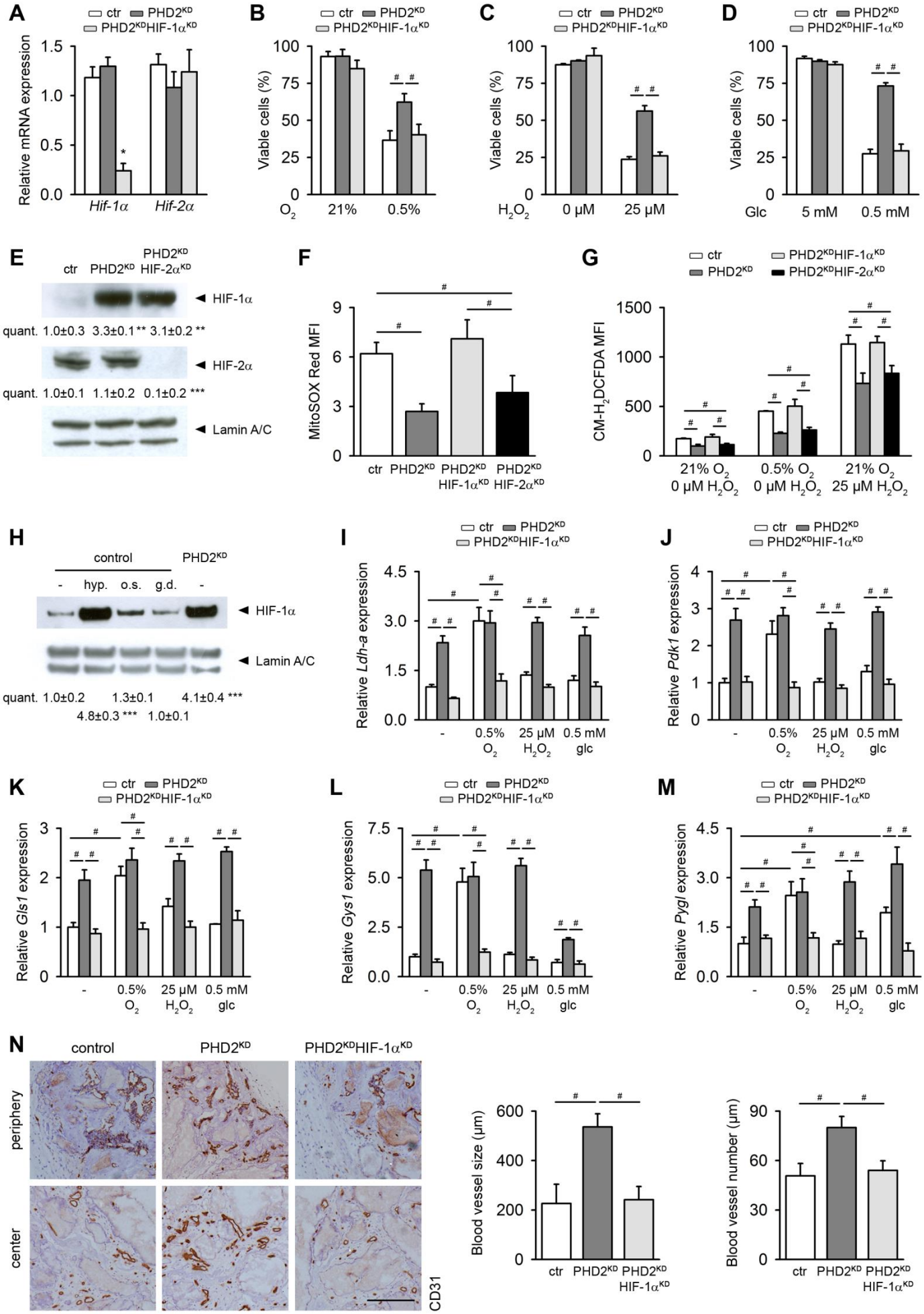
A
ctr
PHD2KD
PHD2KDHIF-1αKD
Relative mRNA expression
Hif-1α
Hif-2α
B
Viable cells (%)
O2
21%
0.5%
C
H2O2
0 μM
25 μM
D
Glc
5 mM
0.5 mM
E
HIF-2KD
HIF-1α
quant. 1.0±0.3 3.3±0.1 ** 3.1±0.2 **
HIF-2α
quant. 1.0±0.1 1.1±0.2 0.1±0.2 ***
Lamin A/C
F
MitoSOX Red MFI
HIF-1αKD
HIF-2αKD
G
HIF-2αKD
CM-H2DCFDA MFI
21% O2 0 μM H2O2
0.5% O2 0 μM H2O2
21% O2 25 μM H2O2
H
control
hyp.
o.s.
g.d.
quant. 1.0±0.2 1.3±0.1 4.1±0.4 ***
4.8±0.3 *** 1.0±0.1
I
Relative Ldh-a expression
J
Relative Pdk1 expression
K
Relative Gls1 expression
L
Relative Gys1 expression
M
Relative Pygl expression
N
periphery
center
CD31
Blood vessel size (μm)
Blood vessel number (μm)

Figure S7, Related to Figure 6. HIF-1α Mediates the Effects in PHD2^{KD} cells

(A) *Hif-1α* and *Hif-2α* mRNA levels in cultured control (ctr), PHD2^{KD} and PHD2^{KD} cells after silencing of HIF-1α (PHD2^{KD}HIF-1α^{KD}) (n=6).

(B-D) Cell viability analysis on cells cultured in single stress conditions (hypoxia (0.5% O_2; B), glucose deprivation (0.5 mM Glc; C) or oxidative stress (25 μM H_2O_2; D)). Viable cells are AnxV$^-$PI$^-$ (n=6).

(E) HIF-1α, HIF-2α and Lamin A/C immunoblot. The ratio of HIF-1α and HIF-2α to Lamin A/C is quantified (n=2-3) and representative blots are shown.

(F) Flow cytometry analysis of mitochondrial superoxide levels in ctr, PHD2^{KD} and PHD2^{KD} cells after silencing of HIF-1α or HIF-2α (PHD2^{KD}HIF-1α^{KD} or PHD2^{KD}HIF-2α^{KD}), quantified by MitoSOX Red MFI (n=3).

(G) Flow cytometry analysis of total intracellular ROS levels during basal culture conditions (21% O_2, 0 μM H_2O_2), hypoxia (0.5% O_2, 0 μM H_2O_2) or oxidative stress (21% O_2, 25 μM H_2O_2), quantified by CM-H_2DCFDA MFI (n=3).

(H) HIF-1α and Lamin A/C immunoblot of ctr, PHD2^{KD} and ctr cells cultured in hypoxia (hyp., 0.5% O_2), oxidative stress (o.s., 25 μM H_2O_2) or glucose deprivation (g.d., 0.5 mM glucose). The ratio of HIF-1α to Lamin A/C is quantified (n=2) and representative blots are shown.

(I-M) *Ldh-a* (I), *Pdk1* (J), *Gls1* (K), *Gys1* (L) and *Pygl* (M) mRNA levels in ctr, PHD2^{KD} and PHD2^{KD}HIF-1α^{KD} cells cultured during *in vitro* stress conditions (n=3).

(N) CD31 immunostaining on ectopically implanted scaffolds eight weeks after implantation with quantification of blood vessel size and number in the entire scaffold (scale bar, 500 μm; n=6).

Data are means ± SEM. *p<0.05 vs. ctr, **p<0.01 vs. ctr, ***p<0.001 vs. ctr (Student's *t*-test), $^{\#}$p<0.05 (ANOVA).

Table S1, Related to Figure 6. Relative mRNA Levels of Indicated Genes in Control, PHD2^{KD} and PHD2^{KD} after shRNA-Mediated Silencing of HIF-1α (PHD2^{KD}HIF-1α^{KD}) or HIF-2α (PHD2^{KD}HIF-2α^{KD}).

		control	PHD2^{KD}	PHD2^{KD}HIF-1α^{KD}	PHD2^{KD}HIF-2α^{KD}
HIF signaling	*Hif-1α*	1.00 ± 0.03	0.87 ± 0.09	0.24 ± 0.08*	0.91 ± 0.01
	Hif-2α	1.00 ± 0.19	1.08 ± 0.26	1.24 ± 0.43	0.15 ± 0.03*
	Phd2	1.00 ± 0.20	0.18 ± 0.07*	0.22 ± 0.04*	0.20 ± 0.01*
Glycolysis	*Glut1*	1.00 ± 0.07	4.78 ± 0.42*	1.11 ± 0.33	4.55 ± 0.06*
	Hk2	1.00 ± 0.11	6.39 ± 1.74*	1.02 ± 0.21	6.10 ± 0.17*
	Pfkfb3	1.00 ± 0.26	5.89 ± 0.71*	1.21 ± 0.08	5.57 ± 0.32*
	Tigar	1.00 ± 0.04	0.71 ± 0.09*	1.12 ± 0.16	0.58 ± 0.03*
Lactate production	*Ldh-a*	1.00 ± 0.26	2.34 ± 0.25*	0.65 ± 0.25	1.82 ± 0.11*
	Mct4	1.00 ± 0.13	4.34 ± 1.01*	1.21 ± 0.34	3.43 ± 0.62*
Glutaminolysis	*Gls1*	1.00 ± 0.20	1.95 ± 0.03*	0.87 ± 0.11	2.69 ± 0.53*
Glyconeogenesis	*Pgm*	1.00 ± 0.14	1.76 ± 0.33*	1.00 ± 0.20	1.40 ± 0.03*
	Gys1	1.00 ± 0.17	5.38 ± 1.23*	0.73 ± 0.28	4.81 ± 0.11*
Glycogenolysis	*Pygl*	1.00 ± 0.11	2.11 ± 0.13*	1.16 ± 0.07	2.06 ± 0.15*
ROS scavengers	*Sod1*	1.00 ± 0.01	1.31 ± 0.03*	1.03 ± 0.11	1.33 ± 0.12*
	Sod2	1.00 ± 0.11	1.82 ± 0.04*	1.25 ± 0.01*	0.70 ± 0.07*
	Cat	1.00 ± 0.09	1.79 ± 0.20*	0.90 ± 0.02	1.64 ± 0.33*

Control and PHD2^{KD} cells are transduced with a lentivirus carrying a scrambled shRNA. Data are means ± SEM. *p<0.05 vs. ctr (Student's *t*-test).

Table S2, Related to Figure 7. Relative mRNA Levels of Indicated Genes in Wild-Type Cells with or without Pharmacological Blockade of PHDs.

		control	JNJ-42041935	IOX2
Glycolysis	*Glut1*	1.00 ± 0.09	3.03 ± 0.59*	3.17 ± 0.83*
	Hk2	1.00 ± 0.08	4.37 ± 0.71*	5.49 ± 0.45*
	Pfkfb3	1.00 ± 0.24	6.27 ± 1.11*	6.00 ± 0.85*
	Tigar	1.00 ± 0.21	0.70 ± 0.07*	0.60 ± 0.27*
Lactate production	*Ldh-a*	1.00 ± 0.24	3.11 ± 0.44*	2.48 ± 0.81*
	Mct4	1.00 ± 0.09	4.14 ± 0.62*	3.77 ± 0.59*
Glutaminolysis	*Gls1*	1.00 ± 0.12	2.07 ± 0.35*	1.84 ± 0.33*
Glyconeogenesis	*Pgm*	1.00 ± 0.06	1.85 ± 0.22*	1.72 ± 0.22*
	Gys1	1.00 ± 0.12	5.24 ± 0.62*	6.40 ± 0.61*
Glycogenolysis	*Pygl*	1.00 ± 0.10	1.92 ± 0.24*	1.86 ± 0.04*

Control (ctr) cells are DMSO-treated wild-type cells. Data are means ± SEM. *p<0.05 vs. ctr (Student's *t*-test).

Supplemental Experimental Procedures

Animals

Phd2$^{fl/fl}$ mice (C57BL/6 background) in which exon 2 was flanked by LoxP sites were a kind gift from P. Carmeliet, and were generated as described before (Mazzone et al., 2009). *Phd2*$^{osx-}$ mice were kindly provided by B. Wielockx and were generated by crossing *Phd2*$^{fl/fl}$ mice with *Osx1-GFP::Cre* mice (Singh et al., 2013; Rodda et al., 2006). C57BL/6 and NMRI nu/nu nude mice were purchased from the R. Janvier Breeding Center (Le Genest St. Isle, France). *Phd2*$^{fl/fl}$ mice were bred in conventional conditions in our animal housing facility (Proefdierencentrum Leuven, Belgium). Housing and experimental procedures were approved by the Institutional Animal Care and Research Advisory Committee of the KU Leuven.

Cell Culture

Isolation and Culture of Murine Periosteal Progenitor Cells. Murine periosteal progenitor cells were isolated according to the protocol described previously (van Gastel et al., 2012). Briefly, femurs and tibias were isolated from 7-9 week old male mice and dissected from muscle and connective tissue. Epiphyses were embedded in 5% low melting point agarose (SeaPlaque, Lonza, Belgium). Subsequently, periosteal cells were isolated by a twofold collagenase-dispase digest (3 mg/ml collagenase and 4 mg/ml dispase in αMEM with 2 mM glutaMAX^{TM}-1, containing 1% penicillin/streptomycin; all from Gibco, Life Technologies, Belgium). Cells obtained after 10 minutes of digest were discarded. The cells obtained during the second digest (50 minutes) were passed through a 70 µm nylon mesh, washed and plated in growth medium (αMEM with 2 mM glutaMAX^{TM}-1, containing 1% penicillin/streptomycin and 10% fetal bovine serum; all from Gibco). Upon 80% confluency, cells were trypsinized and reseeded at a 1/3 ratio. All experiments were performed with periosteal cells of passage 3.

Interaction of Periosteal Cells with Endothelial Cells. A coculture system was used to study the interaction of periosteal cells and endothelial cells. First, periosteal cells were seeded at $5x10^4$ cells/cm^2 and after 24 hours, human umbilical cord vein endothelial cells (HUVEC; Lonza) were added at $1x10^4$ cells/cm^2. The coculture system was cultured in periosteal cell growth medium. After 7 days, the endothelial cells were visualized by staining with a mouse-anti-human CD31 primary antibody (Dako, Denmark) and the TSA Cyanine 3 System (NEN, PerkinElmer, USA). The hCD31-positive surface was quantified using the ImageJ software (National Institutes of Health, USA) at 5 locations per well.

Knockdown and Overexpression Strategies

Adenoviral Transduction. To silence PHD2 expression, *Phd2*$^{fl/fl}$ periosteal cells were transduced with adenovirus-Cre (Ad-Cre; Gene Transfer Vector Core, University of Iowa, USA) at a multiplicity of infection (MOI) of 500. As a control, cells were treated with Ad-GFP (Gene Transfer Vector Core) or Ad-RR5 (kindly provided by J. Swinnen) at the same dose. After 24 hours, virus-containing medium was changed to normal culture medium and 48 hours later, cells were used for further experiments.

Lentiviral Transduction. To silence HIF-1α, GLS1, GLS2 and PYGL expression in PHD2^{KD} periosteal cells, we transduced cells, cultured in the presence of 8 µg/ml polybrene (Sigma-Aldrich), with a lentivirus carrying a shRNA against HIF-1α (kindly provided by P. Carmeliet; MOI 10), GLS1 (MISSION™, Sigma-Aldrich, Belgium; MOI 20), GLS2 (MISSION™, Sigma-Aldrich; MOI 20) or PYGL (MISSION™, Sigma-Aldrich; MOI 10). A nonsense scrambled shRNA sequence was used as a negative control. For ectopic overexpression, cells were transduced with a lentivirus carrying a human GLS1 overexpression vector (kindly provided by P. Carmeliet; MOI 10). A nonsense scrambled shRNA sequence was used as a negative control. After 24 hours, virus-containing medium was changed to normal culture medium and 48 hours later, cells were used for further experiments.

Inhibitors and Intermediates of Metabolic Pathways

Bis-2-(5-phenylacetamido-1,2,4-thiadiazol-2-yl)ethyl sulfide (BPTES), glutamate, dimethyl α-ketoglutarate (dimethyl α-KG), citrate, malate, oxaloacetate, 1,4-dideoxy-1,4-imino-d-arabinitol (DAB) and IOX-2 were obtained from Sigma-Aldrich, JNJ-42041935 (JNJ) was from Merck Millipore (Belgium). All treatments with DAB, BPTES and IOX2 were at 10 µM, JNJ was used at 100 µM. Rescue experiments with dimethyl α-KG and glutamate were performed at 0.5 mM; citrate was used at 1.5 mM, and malate and oxaloacetate were used at 5 mM.

Quantitative Real-Time PCR

Total RNA from cultured cells was extracted using the RNeasy® Mini Kit (Qiagen, The Netherlands), according to the manufacturer's instructions. mRNA was reverse transcribed using Superscript II Reverse Transcriptase (Invitrogen, Life Technologies). qRT-PCR was performed on the 7500 Fast Real-Time PCR System (Applied Biosystems, Life Technologies). Specific forward and reverse oligonucleotide primers as well as probes with fluorescent dye (FAM) and quencher (TAMRA) were used (sequences or premade primer set ID numbers are available upon request). Expression levels were analyzed using the $2^{-\Delta\Delta Ct}$ method and were normalized for the expression of the housekeeping gene hypoxanthine-guanine phosphoribosyl transferase (*Hprt*).

Protein Analyses by Western Blot and ELISA

Whole cell lysates and nuclear extracts were prepared as described before (van Gastel et al., 2012; van Gastel et al., 2014). For phosphorylated AMPK and GLS1 Western blot analysis, cells were lysed in Laemli buffer [62.5 mM Tris-HCl buffer (pH 6.8) containing 10% glycerol, 2% SDS, 1x PhosSTOP (Roche) and 1x complete proteinase inhibitor cocktail (Roche)]. Next, lysates were passed through insulin syringe needles (BD Ultra-Fine™ Needle; BD, Belgium) for homogenization. Proteins were separated by SDS-PAGE under reducing conditions and transferred to a nitrocellulose membrane (GE Healthcare, Belgium).

Membranes were blocked with 5% dry milk or bovine serum albumin (Sigma-Aldrich) in Tris-buffered saline with 0.1% Tween-20 for 60 minutes at room temperature and incubated overnight at 4°C with primary antibodies against PHD2 (Novus Biologicals, USA), HIF-1α (Novus Biologicals), HIF-2α (Abcam, UK), phosphorylated AMPK (Threonin 172; Cell Signaling Technologies, USA), AMPK (Cell Signaling Technologies), GLS1 (kindly provided by P. Carmeliet), β-actin (Sigma-Aldrich) and Lamin A/C (Santa Cruz Biotechnologies, USA). Signals were detected by enhanced chemiluminescence (Western Lightning Plus ECL, PerkinElmer) after incubation with appropriate HRP-conjugated secondary antibodies (Dako, The Netherlands).

Proliferation, NF-κB activation, and VEGF and placental growth factor (PlGF) protein levels were quantified by ELISA assays. Proliferation was measured by 5'-bromo-2'-deoxyuridine (BrdU) incorporation, added during the last 4 hours, using the Cell Proliferation Biotrack ELISA system (GE Healthcare). NF-κB transcription factor activation was quantified with the TransAM^{TM} NF-κB p65 Kit (Active Motif, Belgium). VEGF and PlGF protein levels were measured in the culture medium using the mouse VEGF or mouse PlGF DuoSet ELISA Development Kit (R&D systems), respectively. All ELISAs were performed according to manufacturer's instructions and values were normalized to the amount of DNA.

Metabolism Assays

Glycolysis. For measurement of the glycolytic flux, cells were incubated for 2 hours in growth medium containing 0.4 µCi/ml [5-^{3}H]-D-glucose (PerkinElmer). The culture medium was then transferred into glass vials sealed with rubber caps. $^{3}H_2O$ was captured in hanging wells containing a Whatman paper soaked with H_2O over a period of 48 hours at 37°C to reach saturation (Aragones et al., 2008). Radioactivity was determined in the paper by liquid scintillation counting and values were normalized to DNA content.

Glucose Oxidation. For glucose oxidation, cells were incubated for 5 hours in growth medium containing 0.55 µCi/ml [6-^{14}C]-D-glucose. To stop cellular metabolism, 250 µl of a 2 M perchloric acid solution was added and wells were covered with a Whatman paper soaked with 1x hyamine hydroxide. $^{14}CO_2$ released during the oxidation of glucose was absorbed into the paper overnight at room temperature. Radioactivity in the paper was determined by liquid scintillation counting, and values were normalized to DNA content (Schafer et al., 2009).

Oxygen Consumption. The oxygen consumption rate was quantified using an XF24 analyzer (Seahorse Bioscience Europe, Copenhagen, Denmark). Cells were seeded on Seahorse XF24 tissue culture plates. The assay medium was unbuffered DMEM supplemented with 5 mM D-glucose and 2 mM L-glutamine, pH 7.4 (Gibco, Life Technologies). The measurement of oxygen consumption was performed during 10 minute-intervals (2 minutes mixing, 2 minutes recovery, 6 minutes measuring) for 3 hours, and values were normalized to DNA content.

Fatty Acid Oxidation. Palmitate β-oxidation was measured after incubation of the cells with 2 µCi/ml [9,10-^{3}H]-palmitic acid for 2 hours. Then, the culture medium was transferred into glass vials sealed with rubber caps. $^{3}H_2O$ was captured in hanging wells containing a Whatman paper soaked with H_2O over a period of 48 hours at 37°C. Radioactivity in the paper was determined by liquid scintillation counting, and values were normalized to DNA content (Dagher et al., 2001).

Energy Levels. For determination of energy status, cells were harvested in ice cold 0.4 M perchloric acid supplemented with 0.5 mM EDTA. ATP, ADP and AMP were measured using ion-pair reversed phase high-performance liquid chromatography as previously described (Peeters et al., 2011). Energy status was determined by the ratio of ATP over AMP. Intracellular ATP levels were also measured using the ATPlite ATP detection assay

(PerkinElmer) according to the manufacturer's instructions, and values were normalized to DNA content.

Glucose Uptake, and Glucose, Lactate and Glutamine Consumption. For glucose uptake, cells were incubated with 50 µM of the fluorescent D-glucose analogue 2-[N-(7-nitrobenz-2-oxa-1,3-diazol-4-yl)amino]-2-deoxy-D-glucose (2-NBDG; Molecular Probes, Life Technologies) for 2 hours, washed with PBS, and analyzed by flow cytometry using a Gallios^{TM} Flow Cytometer (Beckman Coulter, USA). Glucose uptake was quantified by the mean fluorescence intensity (MFI) using the Kaluza^{TM} software (Beckman Coulter).

Glucose, lactate and glutamine concentration in conditioned medium was measured using Glucose Assay kit, Lactate Assay kit and Glutamine Colorimetric Assay kit (BioVision, USA), respectively. Results were normalized to DNA content.

Glutathione Levels. Cells were homogenized directly into 5-sulfosalicylic acid (5% w/v), centrifuged, and the supernatant was used to measure reduced glutathione (GSH), oxidized glutathione (GSSG) and total glutathione levels (Glutathione Fluorometric Assay Kit, BioVision). Results were normalized to protein content.

Reactive Oxygen Species (ROS) Levels. Intracellular ROS levels were detected by the use of a fluorescent probe dye, CM-H_2DCFDA (Molecular Probes, Life Technologies). Briefly, periosteal cells were incubated with 10 µM CM-H_2DCFDA for 30 minutes at 37°C, and fluorescence was detected by flow cytometry.

To quantify mitochondrial superoxide production, MitoSOX Red was used. Cells were incubated with 2.5 µM MitoSOX Red for 10 minutes at 37°C, and fluorescence was detected by flow cytometry. Intracellular and mitochondrial ROS levels were expressed as CM-H_2DCFDA and MitoSOX Red MFI, which was calculated by the use of Kaluza^{TM} software.

Glycogen Content. Glycogen levels were measured using the Glycogen Assay Kit (BioVision) following manufacturer's instructions. Briefly, cells were homogenized with 200 µl of distilled water on ice and then boiled for 5 minutes. Homogenates were centrifuged and the supernatants were assayed for glycogen content. Results were normalized to protein content.

A periodic acid-Schiff (PAS) staining was used to visualize glycogen depositions in the cytoplasm. Periosteal cells grown on coverslips were fixed in 4% paraformaldehyde, washed in PBS and incubated in 0.5% periodic acid (Thermo Fisher Scientific, USA) for 5 minutes. Next, cells were washed in distilled water for 5 minutes and incubated in Schiff's reagent (Sigma-Aldrich) for 15 minutes, washed in distilled water for 5 minutes, counterstained with hematoxylin for 1 minute, washed with distilled water for 5 minutes, dehydrated, and mounted.

Liquid Chromatography-Mass Spectrometry (LC-MS) Glutathione Analysis. Samples were extracted in 150 µl 5% trichloroacetic acid, the extract was centrifuged for 10 minutes at 20,000xg. The supernatant was transferred to a vial, 80 µl was injected onto an Acquity UPLC HSS T3 column (2.1x100 mm, particle size 1.8 µm, Waters Corporation, USA) using an Ultimate 3000 UPLC (Thermo Scientific, USA) in-line connected to a Q-Exactive OrbiTRAP mass spectrometer (Thermo Scientific). The column was thermostatted at 37 °C. A linear gradient was carried out using solvent A (0.05% formic acid) and solvent B (60% methanol, 0.05% formic acid). Briefly, 1% solvent B was maintained for 10 minutes, then increased to 100% B at 12 minutes and kept at 100 % B for 3 minutes (t=15 minutes). The gradient returned to 1% solvent B at 16 minutes and allowed to re-equilibrate until 21 minutes. The flow rate was kept constant at 250 µl/minute. Elution of reduced glutathione (GSH) and oxidized glutathione (GSSG) was observed at respectively 3 and 6 minutes. The MS operated in selected ion monitoring (SIM) mode following isotopic envelope of glutathione with m/z 308.09108 to m/z 318.12516. The mass spectrometer was set to positive ion mode, AGC target of 1e6 ions and a maximum injection time of 50 ms. The

sheath gas flow was set at 35, the auxiliary gas flow rate at 10. The spray voltage was used at 3.00 kV and the capillary was heated at 350°C. Auxiliary gas heater temperature was placed at 300°C. Isotope values were corrected for natural abundance according to the method of Fernandez et al. (Fernandez et al., 1996) using in-house developed software.

Gas Chromatography-Mass Spectrometry (GC-MS) Analysis of Glycolytic and TCA Cycle Intermediates. Metabolites for subsequent MS analysis were prepared by quenching the cells in liquid nitrogen followed by a cold two-phase methanol-water-chloroform extraction (Fendt et al., 2013). Phase separation was achieved by centrifugation at 4°C and the methanol-water phase containing polar metabolites was separated and dried using a vacuum concentrator (Fendt et al., 2013). The dried metabolite samples were stored at -80°C. Polar metabolites were derivatized for 90 minutes at 37°C with 7.5 µl of 20 mg/ml methoxyamine in pyridine and subsequently for 60 minutes at 60°C with 15 µl of N-(tert-butyldimethylsilyl)-N-methyl-trifluoroacetamide, with 1% tert-butyldimethylchlorosilane (Fendt et al., 2013). Isotopomer distributions and metabolite levels were measured with a 7890A GC system (Agilent Technologies, Inc., USA) combined with a 5975C Inert MS system (Agilent Technologies, Inc.). One microliter of sample was injected onto a DB35MS column in splitless mode using an inlet temperature of 270°C (Fendt et al., 2013). The carrier gas was helium with a flow rate of 1 ml/minute. Upon injection, the GC oven was held at 100°C for 3 minutes and then ramped to 300°C with a gradient of 2.5°C/minute. The MS system was operated under electron impact ionization at 70 eV and a mass range of 100-650 amu was scanned. Isotopomer distributions were extracted from the raw ion chromatograms using a custom Matlab M-file, which applies consistent integration bounds and baseline correction to each ion (Antoniewicz et al., 2007). In addition, we corrected for naturally occurring isotopes using the method of Fernandez et al. (Fernandez et al., 1996). Total contribution of ^{13}C to a metabolite was calculated as described in Buescher et al. (Buescher et al., 2015).

Cell Viability Assays

In vitro cell viability was detected with Annexin V propidium iodide (AnxV-PI) staining (Annexin V Alexa Fluor® 488 & propidium iodide Dead Cell Apoptosis kit, Molecular Probes, Life Technologies). For single stress conditions, cells were cultured for 72 hours in hypoxia (0.5% oxygen) or in glucose-deprived medium (0.5 mM glucose), or for 12 hours in the presence of hydrogen peroxide (H_2O_2, 25 µM; Sigma-Aldrich). For combined deprivation, cells were cultured in 1% oxygen in medium with 1 mM glucose for 72 hours and 12 µM H_2O_2 was added during the last 12 hours. After harvesting, cells were washed with PBS, incubated with 1x AnxV and 1 µg/ml PI at room temperature for 15 minutes, analyzed by flow cytometry and the percentage of viable cells ($AnxV^-PI^-$) was calculated using Kaluza™ software.

Bone Regeneration Models

To investigate ectopic bone formation, $1x10^6$ periosteal cells were seeded onto NuOss scaffolds (3x3x3 mm^3; ACEuropa, Portugal), incubated overnight, and implanted subcutaneously on the back of female NMRI nu/nu mice. Eight weeks after implantation, scaffolds were retrieved and processed for histology.

To assess the bone forming capacity at an orthotopic location, we used a recently developed non-healing bone defect model in the mouse tibia (van Gastel et al., 2014). Here, $1x10^6$ periosteal cells were seeded onto NuOss scaffolds (2.5x2.5x5 mm^3), incubated overnight, and implanted in a 4 mm mid-diaphyseal bone defect in female NMRI nu/nu mice. Eight weeks after implantation, scaffolds were retrieved and processed for micro-computed tomography (microCT) scans and histology.

***In Vivo* Cell Survival and Metabolic Assays**

To investigate *in vivo* cell survival, we used the ectopic and non-healing bone defect model. Three days after implantation, scaffolds were retrieved and apoptotic cells were detected using immunohistochemical staining for terminal deoxynucleotidyl transferase dUTP nick end labeling (TUNEL) or by *ex vivo* AnxV-PI flow cytometry analysis. For flow cytometry,

cells were isolated from the scaffolds using collagenase-dispase digest for 20 minutes, collected by centrifugation and stained with 1x AnxV allophycocyanin (APC) conjugate (Molecular Probes, Life Technologies) and 1 µg/ml PI (Molecular Probes, Life Technologies). To distinguish implanted cells from host cells, periosteal cells were labeled with CellTracker CM-FDA prior to seeding. Viability of the implanted cells (CM-FDA^{+}AnxV^{-}PI^{-}) was measured using flow cytometry and calculated using Kaluza^{TM} software.

To assess the importance of *in vivo* metabolic adaptations for bone regeneration, we used the ectopic implantation model. Before implantation, cells were labeled with CellTracker CMRA (Molecular Probes, Life Technologies) to distinguish them from host cells. Three days after implantation, scaffolds were retrieved, cells were collected by enzymatic digest and CMRA^{+} cells were sorted by flow cytometry (BD FACSAria III, BD Biosciences, USA). Cytoplasmic ROS levels, the GSH:GSSG ratio and (p-)AMPK protein levels were determined as described above.

To investigate metabolic alterations in *Phd2*$^{osx-}$ mice, we isolated the osteogenic fraction from long bones. Briefly, tibiae and femurs were dissected from the mice and cleaned from muscle and connective tissue. Epiphyses were cut, bone marrow was flushed with PBS and bones were chopped into smaller pieces. Osteogenic cells were isolated using collagenase-dispase digest, on which HIF-1α protein levels and cytoplasmic ROS levels were determined as described above. For determination of the glycogen content and the GSH:GSSG ratio, chopped bone pieces were minced in liquid nitrogen and diluted in the appropriate extraction buffer, as described above.

(Immuno)Histochemistry and Histomorphometry

Isolated scaffolds were fixed in 2% paraformaldehyde overnight and decalcified in EDTA for 14 days, embedded in NEG-50^{TM} frozen section medium (Thermo Fisher Scientific) and sectioned with a cryostat at 7 µm. Histochemical (H&E) and immunohistochemical CD31, TUNEL and Hypoxyprobe-1 stainings were described previously (Maes et al., 2012; van Gastel et al., 2012; van Gastel et al., 2014). To detect apoptotic cells, TUNEL staining

was performed with an *In Situ* Cell Death Detection kit (Roche, Belgium). Hypoxic regions were stained using the Hypoxyprobe-1 PLUS kit after injecting the mice with pimonidazole (Natural Pharmacia International, USA) according to the manufacturer's protocol. Oxidative DNA damage was detected using an 8-hydroxydeoxyguanosine (8-OHdG) antibody (Abcam).

Micro-Computed Tomography

We performed microCT analysis of the newly formed bone using a desktop micro-tomographic image system and related software, as described before (van Gastel et al., 2014). Briefly, retrieved tibias with implanted scaffolds were scanned using the SkyScan 1172 microCT system (Bruker) at a pixel size of 5 µm with 50 kV tube voltage and 0.5 mm aluminum filter. Projection data was reconstructed using the NRecon software (Bruker) and new bone was visualized using custom-made MeVisLab software (MeVis Medical Solutions AG).

Chromatin immunoprecipitation

Cultured cells were fixed using 1% formaldehyde, washed and collected by centrifugation. The pellet was resuspended in RIPA buffer (50 mM Tris-HCl pH 8, 150 mM NaCl, 2 mM EDTA, 1% Triton-X100, 0.5% sodium deoxycholate, 1% SDS, 1% protease inhibitors), homogenized, incubated on ice for 10 minutes and sonicated. The samples were centrifuged and from the supernatant, shared chromatin (1/30) was used as "input" and primary ARNT/HIF-1β monoclonal antibody (NB100-124, Novus Biologicals, USA) was added to the remainder of the chromatin (1/300), and incubated overnight at 4°C. After precipitation using Pierce Protein A/G Magnetic Beads (Life Technologies), RNA and protein digestion, DNA was purified using Agencourt AMPure XP (Beckman Coulter) according to the manufacturer's instructions. RT-qPCR was performed using SYBR® GreenER™ qPCR SuperMix Universal (Life Technologies) and primers (IDT, Leuven, Belgium) for gene-specific HIF binding sites were used.

Gene	Forward primer	Reverse primer
Gls1	5'-GAGAAGGACGACTGACGTGTG-3'	5'-CCTGGTGAATGGCCAGACT-3'
Gys1	5'-GATCCCTTCCCTCTCTGTCC-3'	5'-TTCTACGCAGCATGGAAGTG-3'
Ldh-a	5'-CGACTCACACGTGGGTTCC-3'	5'-AGGGGCCTTAAGTGGAACAG-3'
Pdk1	5'-GCCTACATGGGCGTGTCTTT-3'	5'-ACGGACAGCACGGAGGAG-3'
Pygl	5'-GTCTCTCGGTGTGGAAGGAG-3'	5'-TGGAACCCACTGAGAAGAGG-3'
Background 1	5'-CACTTGCTGAATAATTGGGTTGT-3'	5'-CTGTTGTCCAGTTTTCTTCACG-3'
Background 2	5'-TCTTCCTGCCTTCTTTTGGA-3'	5'-GCTTCCGCTGGTAAGAGTTG-3'

Oligonucleotide sequences used in ChIP-qPCR.

As a positive control, two primers amplifying binding sites of described HIF-1α target genes (*Pdk1* and *Ldh-a*) were used; and two primers amplifying unrelated regions on chromosomes 1 (*Background 1*) and 18 (*Background 2*), which did not contain HIF binding motifs, were selected to assess the background signal. Fold-enrichment for the HIF-1β-ChIP over the input was expressed relative to this background.

Supplemental References

Antoniewicz,M.R., Kelleher,J.K., and Stephanopoulos,G. (2007). Elementary metabolite units (EMU): a novel framework for modeling isotopic distributions. Metab Eng *9*, 68-86.

Aragones,J., Schneider,M., Van Geyte,K., Fraisl,P., Dresselaers,T., Mazzone,M., Dirkx,R., Zacchigna,S., Lemieux,H., Jeoung,N.H., Lambrechts,D., Bishop,T., Lafuste,P., Diez-Juan,A., Harten,S.K., Van Noten,P., De Bock,K., Willam,C., Tjwa,M., Grosfeld,A., Navet,R., Moons,L., Vandendriessche,T., Deroose,C., Wijeyekoon,B., Nuyts,J., Jordan,B., Silasi-Mansat,R., Lupu,F., Dewerchin,M., Pugh,C., Salmon,P., Mortelmans,L., Gallez,B., Gorus,F., Buyse,J., Sluse,F., Harris,R.A., Gnaiger,E., Hespel,P., Van Hecke,P., Schuit,F., Van Veldhoven,P., Ratcliffe,P., Baes,M., Maxwell,P., and Carmeliet,P. (2008). Deficiency or inhibition of oxygen sensor Phd1 induces hypoxia tolerance by reprogramming basal metabolism. Nat. Genet. *40*, 170-180.

Buescher,J.M., Antoniewicz,M.R., Boros,L.G., Burgess,S.C., Brunengraber,H., Clish,C.B., DeBerardinis,R.J., Feron,O., Frezza,C., Ghesquiere,B., Gottlieb,E., Hiller,K., Jones,R.G., Kamphorst,J.J., Kibbey,R.G., Kimmelman,A.C., Locasale,J.W., Lunt,S.Y., Maddocks,O.D., Malloy,C., Metallo,C.M., Meuillet,E.J., Munger,J., Noh,K., Rabinowitz,J.D., Ralser,M., Sauer,U., Stephanopoulos,G., St-Pierre,J., Tennant,D.A., Wittmann,C., Vander Heiden,M.G., Vazquez,A., Vousden,K., Young,J.D., Zamboni,N., and Fendt,S.M. (2015). A roadmap for interpreting C metabolite labeling patterns from cells. Curr. Opin. Biotechnol. *34C*, 189-201.

Dagher,Z., Ruderman,N., Tornheim,K., and Ido,Y. (2001). Acute regulation of fatty acid oxidation and amp-activated protein kinase in human umbilical vein endothelial cells. Circ. Res. *88*, 1276-1282.

Fendt,S.M., Bell,E.L., Keibler,M.A., Olenchock,B.A., Mayers,J.R., Wasylenko,T.M., Vokes,N.I., Guarente,L., Vander Heiden,M.G., and Stephanopoulos,G. (2013). Reductive glutamine metabolism is a function of the alpha-ketoglutarate to citrate ratio in cells. Nat. Commun. *4*, 2236.

Fernandez,C.A., Des Rosiers,C., Previs,S.F., David,F., and Brunengraber,H. (1996). Correction of 13C mass isotopomer distributions for natural stable isotope abundance. J. Mass Spectrom. *31*, 255-262.

Maes,C., Araldi,E., Haigh,K., Khatri,R., Van Looveren,R., Giaccia,A.J., Haigh,J.J., Carmeliet,G., and Schipani,E. (2012). VEGF-independent cell-autonomous functions of HIF-1alpha regulating oxygen consumption in fetal cartilage are critical for chondrocyte survival. J. Bone Miner. Res. *27*, 596-609.

Mazzone,M., Dettori,D., Leite de Oliveira,R., Loges,S., Schmidt,T., Jonckx,B., Tian,Y.M., Lanahan,A.A., Pollard,P., Ruiz de Almodovar,C., De Smet,F., Vinckier,S., Aragones,J., Debackere,K., Luttun,A., Wyns,S., Jordan,B., Pisacane,A., Gallez,B., Lampugnani,M.G., Dejana,E., Simons,M., Ratcliffe,P., Maxwell,P., and Carmeliet,P. (2009). Heterozygous deficiency of PHD2 restores tumor oxygenation and inhibits metastasis via endothelial normalization. Cell *136*, 839-851.

Peeters,A., Fraisl,P., van den Berg,S., Ver Loren van Themaat,E., Van Kampen,A., Rider,M.H., Takemori,H., van Dijk,K.W., Van Veldhoven,P.P., Carmeliet,P., and Baes,M. (2011). Carbohydrate metabolism is perturbed in peroxisome-deficient hepatocytes due to mitochondrial dysfunction, AMP-activated protein kinase (AMPK) activation, and peroxisome proliferator-activated receptor gamma coactivator 1alpha (PGC-1alpha) suppression. J. Biol. Chem. *286*, 42162-42179.

Rodda,S.J. and McMahon, A.P. (2006). Distinct roles for Hedgehog and canonical Wnt signaling in specification, differentiation and maintenance of osteoblast progenitors. Development *133*, 3231-3244.

Schafer,Z.T., Grassian,A.R., Song,L., Jiang,Z., Gerhart-Hines,Z., Irie,H.Y., Gao,S., Puigserver,P., and Brugge,J.S. (2009). Antioxidant and oncogene rescue of metabolic defects caused by loss of matrix attachment. Nature *461*, 109-113.

Singh,R.P., Franke,K., Kalucka,J., Mamlouk,S., Muschter,A., Gembarska,A., Grinenko,T., Willam,C., Naumann,R., Anastassiadis,K., Stewart,F.A., Bornstein,S., Chavakis,T., Breier,G., Waskow,C., and Wielockx,B. (2013). HIF prolyl hydroxylase 2 (PHD2) is a critical regulator of hematopoietic stem cell maintenance during steady-state and stress. Blood *121*, 5158-5166.

van Gastel,N., Stegen,S., Stockmans,I., Moermans,K., Schrooten,J., Graf,D., Luyten,F.P., and Carmeliet,G. (2014). Expansion of murine periosteal progenitor cells with fibroblast growth factor 2 reveals an intrinsic endochondral ossification program mediated by bone morphogenetic protein 2. Stem Cells *32*, 2407-2418.

van Gastel,N., Torrekens,S., Roberts,S.J., Moermans,K., Schrooten,J., Carmeliet,P., Luttun,A., Luyten,F.P., and Carmeliet,G. (2012). Engineering vascularized bone: osteogenic and proangiogenic potential of murine periosteal cells. Stem Cells *30*, 2460-2471.